Synthesis of Magnetic Spherical Polyelectrolyte Brushes

ARTICLE *in* MACROMOLECULES · JANUARY 2011

Impact Factor: 5.8 · DOI: 10.1021/ma102337c

632 *Macromolecules* **2011**, *44*, 632–639
DOI: 10.1021/ma102337c

Macromolecules
ARTICLE

Synthesis of Magnetic Spherical Polyelectrolyte Brushes

Kaimin Chen,[†] Yan Zhu,[†] Yifei Zhang,[†] Li Li,[†] Yan Lu,[‡] and Xuhong Guo*,[†]

[†]*State Key Laboratory of Chemical Engineering, School of Chemical Engineering, East China University of Science and Technology, Shanghai 200237, China, and* [‡]*German Soft Matter and Functional Materials, Helmholtz-Zentrum Berlin für Materialien und Energie GmbH, Berlin 14109, Germany*

Received October 13, 2010; Revised Manuscript Received December 27, 2010

ABSTRACT: Magnetic spherical polyelectrolyte brushes (MSPB) with embedded magnetite nanoparticles in core were successfully synthesized and characterized by dynamic light scattering (DLS), a scanning electron microscope (SEM), a high resolution transmission electron microscope (HRTEM), thermal gravimetric analysis (TGA), X-ray diffraction (XRD), and a vibrating sample magnetometer (VSM). At first, oleic acid modified magnetite nanoparticles (MNP) were synthesized by the coprecipitation method and then embedded into the polystyrene core by miniemulsion polymerization to obtain magnetic polystyrene latices (MPL). Finally, magnetic spherical poly(acrylic acid) (PAA) brushes were synthesized by photoemulsion polymerization. Effects of MNP and acrylic acid (AA) content on the brush structure were studied in detail. The obtained MSPB are narrowly dispersed, pH sensitive, superparamagnetic, and redispersible after aggregating by external magnetic field. Magnetic control is thus introduced into nanosized spherical polyelectrolyte brushes to achieve the recovery and controllable delivery. This approach opens a new way for the recoverable and cost-effective applications of spherical polyelectrolyte brushes.

Introduction

The area of polyelectrolyte brushes is one of the most active research fields in polymer science.[1] Spherical polyelectrolyte brushes (SPB), serving as a simple model between star polyelectrolyte[2] and planar polyelectrolyte brushes,[3,4] are extremely useful in both fundamental science and industrial applications.[5] As smart nanoparticles, SPB have been used for adsorption of proteins,[6,7] ideal carrier for high-efficiency catalyst,[8,9] and synthesis of metal nanoparticles.[10,11] The nanosized SPB are very stable in water due to the steric protection and the electrostatic repulsion of polyelectrolyte brush layer, while their recycle after application becomes quite difficult. Therefore, it is highly desirable for the applications of SPB to possess a tunable stability and mobility that can be conveniently controlled by external stimuli such as magnetic field.

Recently, magnetic nanoparticles (MNP), especially magnetite nanoparticles, attract a growing interest.[12−18] Compared with their bulk counterparts, the main advantages of MNP lie in high specific surface areas, low sedimentation rate, reduced magnetic dipole−dipole interactions, which pronounce a promising future in drug or gene delivery,[19] magnetic resonance imaging[20] and hyperthermia.[21] To avoid the aggregation of MNP, their surfaces are normally modified by polymers[22−31] or inorganic materials[32−34] to obtain necessary stability for applications.

Among methods to modify MNP surface, polymers can be covered onto a single MNP by physical absorption[35] or in situ polymerizations such as surface-initiated atom transfer radical polymerization (ATRP).[36−39] MNP also can be embedded into polymer matrices by in situ polymerization[40−43] or encapsulated by polyorganosiloxane by polycondensation reaction[44,45] to form magnetic composite particles with controllable size and magnetite content. However, to the best of our knowledge, it is still a challenge to control the surface structure of polymers and the size distribution of particles.

*To whom correspondence should be addressed. Telephone: +86 21 6425 3491. Fax: +86 21 6425 3491. E-mail: guoxuhong@ecust.edu.cn.

In this work, we demonstrate a novel approach to prepare narrowly dispersed polymer/magnetite nanocomposite particles with well-controlled surface and particle size. These magnetic spherical polyelectrolyte brushes (MSPB) consist of a polystyrene (PS) core around 100 nm in diameter embedded with magnetite nanoparticles and a well-defined shell of poly(acrylic acid) (PAA) brush (Scheme 1). The magnetic properties, the brush thickness and the grafting density of PAA chains on the core surface are tunable by controlling the dose of MNP, acrylic acid (AA) and the photoinitiator 2[*p*-(2-hydroxy-2-methylpropiophenone)]−ethylene glycol−methacrylate (HMEM), respectively (Scheme 1). Magnetic polystyrene latices (MPL) are synthesized via miniemulsion polymerization and MSPB by photoemulsion polymerization. The introduction of surface modified MNP into SPB core makes it possible to recycle SPB magnetically and redisperse after removing external magnetic field.

Experimental Section

1. Materials. Ferric chloride hexahydrate ($FeCl_3 \cdot 6H_2O$), ferrous sulfate heptahydrate ($FeSO_4 \cdot 7H_2O$) and anhydrous ethyl alcohol were purchased from Sinopharm Chemical Reagent Co., Ltd. Oleic acid (OA), sodium dodecyl sulfate (SDS), *n*-octane, acetone, ammonium hydroxide (25 wt %), hydrochloride acid (36 wt %), potassium persulfate (KPS) and pyridine were bought from Lingfeng Chemical Reagent Co., Ltd. Hexadecane (99%) was purchased from Acros Organics and methacryloyl chloride (MC) from Technical Choices, Inc. The 2-hydroxy-4′-hydroxyethoxy-2-methylpropiophenone (HMP) (Irgacure 2959) was kindly donated by Ciba Specialty Chemicals Inc. All these chemicals were used without further purification. The 2,2′-azo-bis-iso-butyronitrile (AIBN) (from Shanghai No.4 Reagent & H.V. Chemical Company) was recrystallized in methanol before use. Styrene and acrylic acid (AA) (from Shanghai Lingfeng Chemical Regent Co., Ltd.) were distilled under reduced pressure and stored in refrigerator at 4 °C before use. The water used in all experiments was purified by reverse osmosis (Shanghai RO Micro Q).

 Published on Web 01/12/2011

Scheme 1. Schematic Illustration of the Synthesis of MSPB

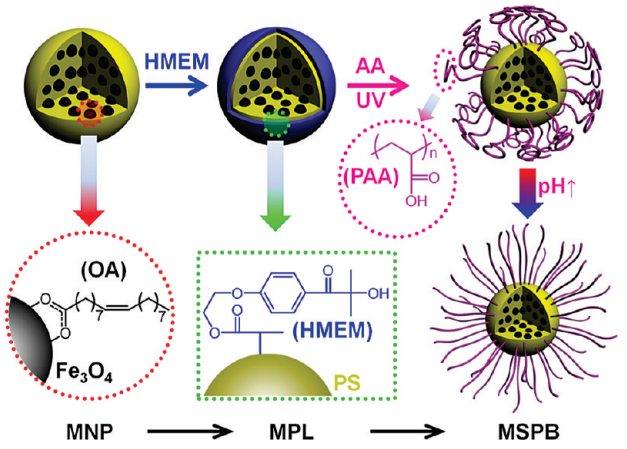

2. Preparation of Magnetite Nanoparticles (MNP). Magnetic nanoparticles were synthesized by coprecipitation method in the presence of oleic acid (OA). In a typical run, 48.60 g of $FeCl_3 \cdot 6H_2O$ and 33.36 g of $FeSO_4 \cdot 7H_2O$ with a molar ratio of 3:2 were dissolved in water and heated to 90 °C under vigorous stirring. 23.2 g of OA was dissolved in 25 mL of acetone and added to the reaction system followed by 120 mL of ammonia solution. After 2 h, the sediment was neutralized by 1 N hydrochloride acid. Then anhydrous ethyl alcohol was introduced to get rid of the residual OA. Finally the byproduct ammonium chloride was eluted by water from the black sediment. A black product was collected with the help of a magnet and dried in lyophilizer for 24 h. Dried MNP were stored at room temperature or dispersed in *n*-octane with a concentration of 62.5 wt % to form a magnetic fluid for further use.

3. Synthesis of Magnetic Polystyrene Latices (MPL). Magnetic polystyrene latices were synthesized by miniemulsion polymerization. In the case of using AIBN as initiator, 0.10 g of hexadecane, 0.075 g of AIBN and 2.50 g of styrene were mixed with a certain amount of MNP followed by ultrasonication for 15 min in an ice bath. The ultrasonication device is Model SK7210LHC from KUDOS Co. with the highest frequency of 53 kHz and power of 350 W. The obtained oil phase was added into 200 mL of SDS solution (0.1 wt %) followed by miniemulsification for 60 min in an ice bath. Miniemulsion polymerization was then started at 65 °C and performed for 20 h under stirring of 300 rpm. At the end of the miniemulsion polymerization, 4.5 g of acetone solution with 0.5 g of photoinitiator HMEM synthesized in our laboratory[46] was added in 30 min under "starved condition". MPL with a thin layer of HMEM were thus obtained after further 2.5 h reaction.

In the case of using KPS as initiator, the required amount of MNP magnetic fluid was added to SDS solution and mixed by ultrasonication for 60 min in an ice bath to form MNP clusters. Then, 2.50 g of styrene and 0.10 g of hexadecane (as costabilizer) was added followed by another 60 min ultrasonication. Miniemulsion polymerization was then performed after adding 0.05 g of KPS at 80 °C for 20 h under stirring of 300 rpm. HMEM was introduced with the same procedure as described above.

4. Synthesis of Magnetic Spherical Polyelectrolyte Brushes (MSPB). MPL were charged into a homemade UV-reactor (range of wavelengths: 200−600 nm, power: 150 W), and diluted to 0.5 wt % with water until the total weight reached 500 g. A defined amount of acrylic acid (AA) was added. The whole reactor was degassed by repeated evacuation and subsequent addition of nitrogen at least three times. Photoemulsion polymerization was accomplished with UV radiation at room temperature with vigorous stirring in 2.5 h. The obtained MSPB emulsion was purified exhaustively by dialysis against water until the conductance of the eluate did not change anymore.

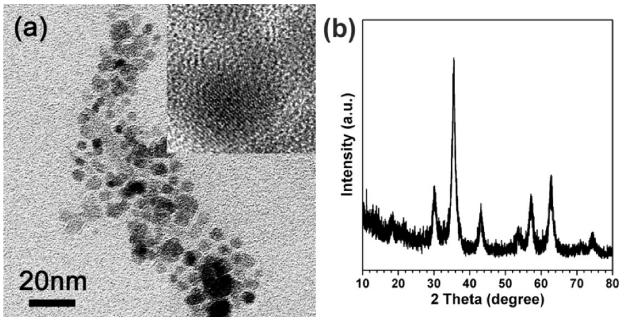

Figure 1. Characterization of MNP: (a) TEM image, where the inset shows the HRTEM image of a single MNP; (b) XRD spectrum of MNP.

5. Characterization. Dynamic light scattering (DLS) was used to determine the apparent hydrodynamic size of particles and performed by a particle sizing system of NICOMP 380 ZLS at a fixed scattering angle of 90°. Without extrapolation to zero scattering angle, the apparent hydrodynamic radius obtained by DLS at 90° should be smaller than the true one. X-ray diffraction (XRD) were carried out on a Bruker D8 Advance X-ray diffractometer with a scan rate of 6° /min. Thermal gravimetric analysis (TGA) WRT-2P was employed to determine the magnetite content in particles. The high resolution transmission electron microscopy (HRTEM) was performed using a JEOL-2100F electron microscope operating at 200 kV. Samples were magnetically separated before TEM observation. The magnetic properties of samples were characterized by vibrating sample magnetometer (VSM) of Lakeshore 7407 at room temperature. Turbidity was monitored with a Brinkman PC 950 colorimeter equipped with a 2 cm path length optical probe.

Results and Discussion

1. Magnetic Property. *1.1. Magnetite Nanoparticles.* Magnetite nanoparticles modified by OA (MNP) were synthesized by coprecipitation route.[15,47−54] As shown in Figure 1a, the obtained MNP are around 10 nm. The crystal lattice can be clearly seen in the HRTEM image of a single MNP while the surface becomes fuzzy due to the small-size effect of nanoparticles.[55] The crystal structure of MNP was also confirmed by XRD (Figure 1b). The six characteristic peaks of magnetite at 30.2° (220), 35.5° (311), 43.2° (400), 53.6° (422), 57.2° (511), and 62.8° (440) can be determined, and the calculated diameter from XRD patterns by Scherrer's formula[56] is 9.5 nm, which is consistent with the size observed in TEM image. OA was adsorbed on MNP surface via coordination interaction between carboxylate group in oleic acid and iron atom.[54] OA content was ca. 25 wt % as determined by TGA.

1.2. MNP in MSPB. In the first instance, we used the conventional emulsion polymerization to embed MNP into polystyrene core. However, the magnetite content in obtained yellowish MPL was below 2 wt % as determined by TGA, which was not sufficient for magnetic separation. The similar results were reported in literatures.[57,58] Therefore, we turned to employ miniemulsion polymerization method[22,24,26,28,59,60] to introduce more MNP into polystyrene core. Followed this strategy, MPL with narrow size distribution were synthesized. Poly(acrylic acid) (PAA) brushes were then grown from the surface of MPL via photoemulsion polymerization technique.

Figure 2 shows the HRTEM images of prepared MSPB encapsulating MNP in PS core. Obviously, MNP are successfully embedded in MSPB and mainly locate inside the core. The MSPB show narrow size distribution and well-defined

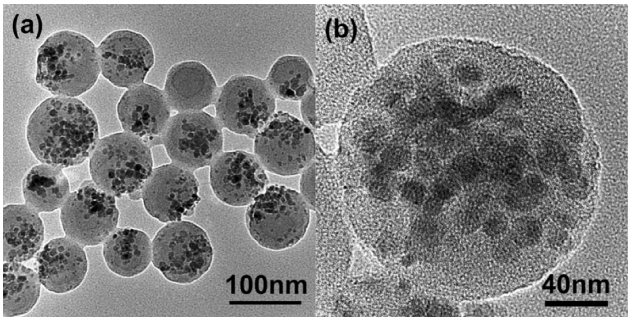

Figure 2. TEM images of as-synthesized MSPB. Their magnetite content is 10.9 wt % determined by TGA.

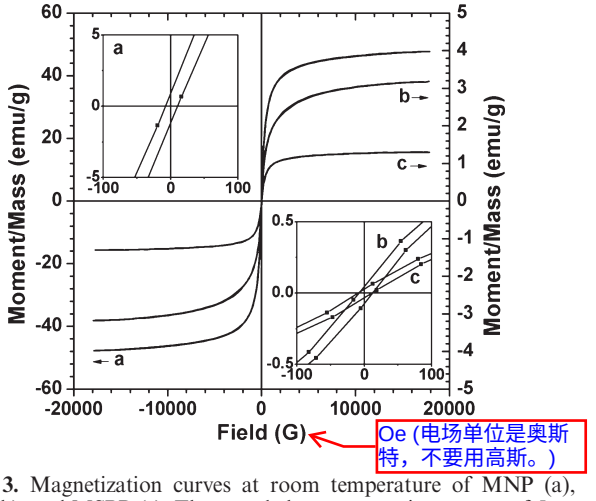

Figure 3. Magnetization curves at room temperature of MNP (a), MPL (b), and MSPB (c). The sample has a magnetite content of 5 wt %. Insets are corresponding magnetization curves at low magnetic field to show residual magnetization and coercive force.

structure although the PAA brush shell can hardly be observed in dry state.

1.3. Hysteresis Loops. Vibrating sample magnetometer (VSM) was employed to compare the magnetic property of synthesized MNP, MPL, and MSPB. As shown in Figure 3, the saturation magnetization value of MNP was 47.7 emu/g at room temperature. Their remanence and coercive force were very small and could be at the range of superparamagnetism.[16,61] The small remanence may come from few relatively large magnetite nanoparticles prepared by coprecipitation method, which should bring limited effect on the overall magnetic properties of MPL and MSPB. After embedding MNP into PS core, the saturation magnetizations of MPL and MSPB reduced to 3.18 and 1.30 emu/g, respectively. Their remanences, calculated from residual magnetization divided by saturation magnetization, were as small as MNP (around 0.02, see Figure 3). The coercive forces of MPL and MSPB were 10.0 and 10.7 Oe, respectively, which should be also within the superparamagnetism range.[62] The saturation magnetization of MNP encapsulated in MSPB is reduced to 26 emu/g of magnetite. The loss of magnetization is probably due to the polymer encapsulation[63] or partial oxidation forming nonmagnetic iron oxide such as α-Fe_2O_3 during the ultrasonication.[23] Therefore, the synthesized MPL and MSPB were still superparamagnetic although their saturation magnetizations were much lower than that of MNP.

2. Brush Structure and Property. *2.1. Ultrasonication and Core Size.* The droplet size before miniemulsion polymerization has strong impact on brush core size. Long time of

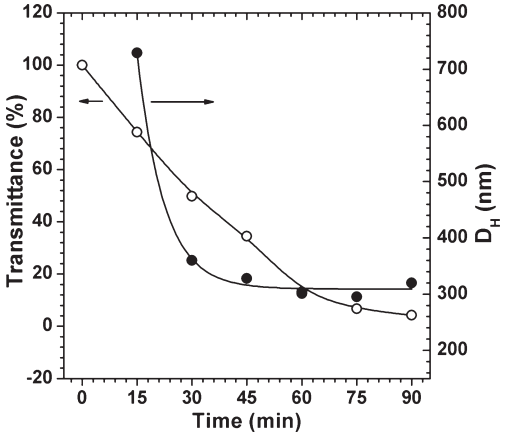

Figure 4. Transmittance (○) and D_H (●) as a function of ultrasonication time during miniemulsification.

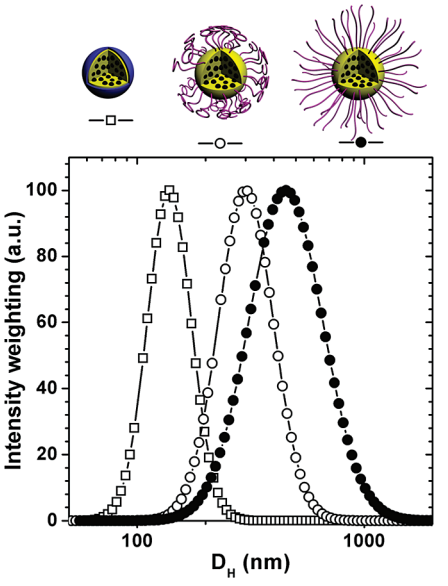

Figure 5. Size and size distribution of MPL (□), MSPB at pH 4 (○) and pH 9 (●) as determined by DLS. The magnetite content of MSPB is 3.9 wt %.

ultrasonication with high power and frequency is favorable to form homogeneous emulsion with small size.[23,64] In our experiments, 53 kHz and 350 W were chosen as the ultrasonication parameters by employing an ultrasonicator SK7210LHC from KUDOS Co. Both the transmittance and apparent hydrodynamic diameter (D_H) of droplets during miniemulsification were monitored by colorimeter and DLS, respectively (Figure 4).

Upon increasing the ultrasonication time, the transmittance decreased gradually and reached a plateau after ca. 60 min, while D_H of droplets decreased dramatically in 30 min followed by a plateau (Figure 4). These results implied that large droplets were broken early and fast in the first 30 min since they had more contribution to the scattering intensity during DLS measurements while the average size of droplets reduced gradually. During ultrasonication, an ice bath was applied to control the temperature in order to obtain MPL with narrow size distribution. The optimal ultrasonication time was 60 min (Figure 4).

2.2. Growing of PAA Brush. The growing of PAA brushes can be monitored from the size change by DLS. The size and size distribution of MSPB with PAA shell are shown in

Table 1. Brush Thickness and Magnetite Content

MSPB	AA[a] (wt %)	L[b] (nm)	PDI[c]	MC[d] (wt %)
A-0	0	0	0.040	6.8
A-1	25	8	0.044	5.0
A-2	50	37	0.010	4.9
A-3	75	110	0.112	4.7
A-4	100	155	0.140	3.9

[a] AA: Content of AA compared with MPL by weight. [b] L: Brush layer thickness of MSPB determined by DLS at pH 9.0. [c] PDI: Polydispersity index of MSPB determined by DLS. [d] MC: Magnetite content in MSPB determined by TGA.

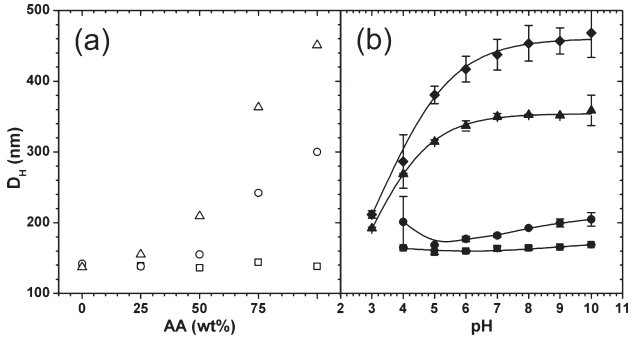

Figure 6. (a) Effect of AA content on size of MSPB. Key: (□) MPL, (○) MSPB at pH 4; (△) MSPB at pH 9. (b) Size of MSPB as a function of pH. Key: (■) 25 wt % AA; (●) 50 wt % AA; (▲) 75 wt % AA; (♦) 100 wt % AA. Lines are to guide the eye.

Figure 5. The D_H of MPL was around 140 nm which was much smaller than droplets before miniemulsion polymerization (Figure 4). This observation is consistent with that of other authors[65] whose explanation is that DLS gave a "wrong size" to nonsolid styrene droplets containing MNP. After grafting of PAA through photoemulsion polymerization, D_H of MSPB increased to 300 nm at pH 4.0 and 450 nm at pH 9.0. PAA grafted MSPB expanded at high pH due to the dissociation of carboxyl groups in PAA and thus the electrostatic repulsion between adjacent PAA chains. The size distribution of MSPB fitted by Gaussian distribution is of a polydispersity index of 0.14 as determined by DLS which is higher than that of MPL. The increase in polydispersity of MSPB may come from the possible agglomerates, especially at high pH when all the PAA are fully extended.

2.3. Brush Thickness and pH Sensitivity. The thickness of SPB brush is tunable by the dose of monomer AA.[46] When MNP were introduced inside SPB, the effect of AA dose on MSPB thickness is shown in Table 1. The size of MPL core is around 140 nm with a polydispersity index of 0.04. Upon increasing the AA dose, the thickness of MSPB increased monotonically while the relative content of magnetite decreased (Table 1). If AA amount is over 100 wt %, MSPB become unstable with a broad size distribution due to the possible cross-linking among them.[46]

Figure 6 displayed the effect of AA content and pH value on the diameter (D_H) of MSPB. Like other PAA SPB without MNP inside the core, MSPB are sensitive to both pH value and ionic strength.[46,66,67] 1 mL of 0.5 wt % MSPB was diluted 100 times by adding into 99 mL of 10 mM NaCl solution. For all the samples, pH decreased from 10.0 by adding 10 mM HCl while the ionic strength kept 10 mM adjusted by NaCl. The size increase of MSPB with pH is due to the increase of the electrostatic repulsion among PAA chains in MSPB. As shown in Figure 6, MSPB with low AA dose are unstable at low pH (pH ≤ 4) because of the inadequate steric protection and reduced electrostatic repulsion.

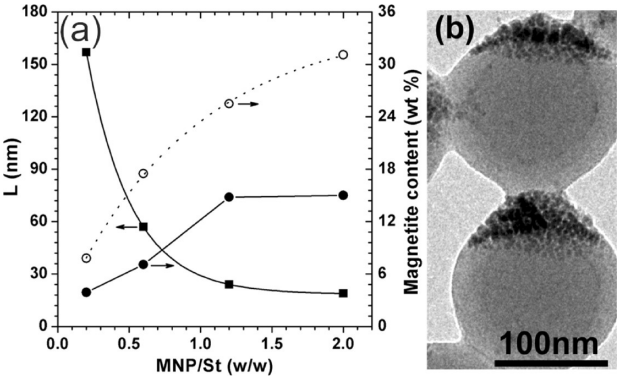

Figure 7. (a) Effect of MNP dose ratio on the thickness of MSPB and magnetite content. Key: (■) brush thickness L; magnetite amount in MSPB as determined (●) by TGA and (○) in theory. (b) TEM image of a sample with magnetite content of 14.8 wt % by TGA.

Table 2. Brush Thickness and Magnetite Content Using AIBN as Initiator

MSPB	MNP/St[a]	AA (wt %)	MPL[b] (nm)	L (nm)	MC (wt %)
A-4	0.2	100	140	157	3.9
A-5	0.6	100	181	57	7.1
A-6	1.2	100	184	24	14.8
A-7	2.0	100	177	19	15.0

[a] MNP/St: Feed ratio of MNP to styrene. [b] MPL: Diameter of polystyrene particles containing magnetite nanoparticles.

3. Morphology Control. The morphology of MPL and the grafting of PAA chains on MPL surface will be affected by the encapsulation of MNP.[68] In our experiments, the employment of different initiators during the miniemulsion polymerization for MPL synthesis was found to have significant impact on the morphology of MSPB.

3.1. Using AIBN. AIBN was selected as the initiator since its oil solubility can effectively reduce secondary nucleation.[69] According to the miniemulsion mechanism, droplets are the main reaction site.[65,70−72] The secondary nucleation and further growing will form much more nonmagnetic SPB in MSPB emulsions, which has negative effects on the encapsulation of MNP particles and size distribution of MPL.

In order to respond quickly to magnetic field for MSPB, more embedded MNP are favorable. If the magnetite content reaches ca. 15 wt %, the magnetic separation time can be reduced to a reasonable value.[73] However, upon increasing the dose of MNP, the thickness of MSPB reduced significantly and reached a plateau of ca. 20 nm when the weight ratio of MNP to styrene approached 1.2 (Figure 7a). The increased amount of MNP is unfavorable to the covalent attachment of photoinitiator on the core surface and thus the growth of PAA brushes.

The magnetite content in MSPB determined by TGA was much lower than that calculated theoretically (Figure 7a). For example, sample A-6 and A-7 had the similar magnetite content in the final MSPB while the dose of MNP for A-6 was only 60% of A-7 (Table 2). We tried even higher dose of MNP than A-7, but the highest magnetite content in MSPB was around 15 wt %. This result accords with the report in literatures where 15 wt % seems to be the upper limit magnetite content if MNP were mixed with styrene without other treatment.[24,26,28] The possible reason is the limited compatibility between PS matrix and hydrophobic OA backbone on the surface of MNP. Therefore, some MNP are easy to lose during the polymerization. This hypothesis has been confirmed in our experiments where black sediments always

can be found at the bottom of flasks at high dose of magnetite content.

Figure 7b showed the typical TEM image of MSPB based on AIBN initiator. Janus particles were observed where the MNP located far away from the particle center. Instead of PS core, we also tried to use poly(methyl methacrylate) (PMMA) core which has improved compatibility with OA modified magnetite nanoparticles.[29] But the obtained particles were irregular in shape.

The acentric phenomenum for MNP in MSPB (Figure 7b) can also be explained by the mechanism of miniemulsion polymerization. The polymerization is initiated and performed inside the magnetic droplets where oil soluble initiator AIBN dissolved (Scheme 2a). As a result, the MNP tend to be pushed aside of the droplet during the polymerization due to the relatively poor compatibility between PS matrix and OA surfactant on the surface of magnetite nanoparticles.

3.2. Using KPS. KPS was an alternative initiator for miniemulsion polymerization.[22,28,29] Although it may bring the secondary nucleation problem, KPS dissolves in water and initiates the polymerization from out to center pushing the MNP to the center of core (Scheme 2b). By choosing the type and optimizing the amount of surfactant, the secondary nucleation problem for KPS can be minimized.[74] Even though the secondary nucleation happens, the formed SPB without MNP can be removed by applying an external magnetic field. Therefore, KPS should be a good choice to improve the encapsulation of MNP.

Additionally, in order to encapsulate more than 15 wt % magnetite in MSPB, which cannot reach by simply using KPS as initiator,[26] MNP clusters were prepared prior to the miniemulsion polymerization. Several methods were reported to prepare MNP clusters.[34,75] We used SDS as surfactant to prepare MNP clusters with the help of ultrasonication.[30,31] As observed by TEM (Figure 8c), the obtained MNP clusters are spherical with an average diameter of 150 nm.

Magnetite content in MSPB determined by TGA is listed in Table 3 and compared with theoretical data (Figure 8a). During the experiment, no black sediments can be found even at high feed ratio of MNP/styrene, which implied that almost all of the MNP were encapsulated into PS core. Compared with MSPB prepared using AIBN as initiator with the same feed ratio of MNP/styrene (Table 2), the MNP content in MSPB (Table 3) enhanced significantly. The highest MNP content in MSPB by using KPS as initiator can reach 52.3 wt %. However, the brush thickness of MSPB also reduced dramatically upon increasing the dose of MNP due to the similar reason as discussed above. Interestingly, the magnetite content of MSPB was higher than theoretical value by following this route (Figure 8a), which was mainly attributed to the reduced polymerization of styrene by deactivation of radicals decomposited by KPS in water and the removal of nonmagnetic SPB from secondary nucleation during magnetic separation.

TEM image in Figure 8b indicated that most MNP locate in the center even at very high dose (Figure 8d). It seems that the MNP content in MSPB can be even higher than 52.3 wt % by using MNP cluster technique.[23] However, the thickness of PAA brush did not increase any more when MNP content reached 52.3 wt % even though we increased the amount of AA monomer and photoinitiator content.

4. Dispersibility. *4.1. Apparent Dispersibility.* As shown in Figure 9, MPL after dialyze against water is unstable and will totally precipitate after standing at room temperature for several minutes, while MSPB are very stable even after several months without sediments. Higher stability of MSPB

Scheme 2. Morphology Change during Miniemulsion Polymerization Using Different Initiators

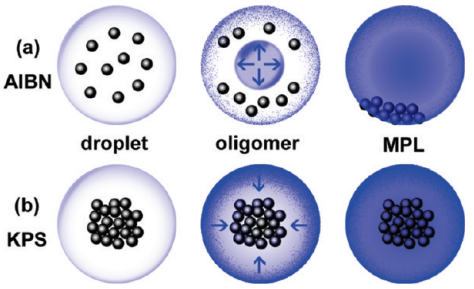

Table 3. Brush Thickness and Magnetite Content Using KPS as Initiator

MSPB	MNP/St	AA (wt %)	MPL (nm)	*L* (nm)	MC (wt %)
K-1	0.015	100	97	107	5.2
K-2	0.08	100	111	60	10.9
K-3	0.17	100	112	26	13.7
K-4	0.2	100	88	14	17.4
K-5	0.4	100	98	17	24.0
K-6	1.2	100	125	25	52.3

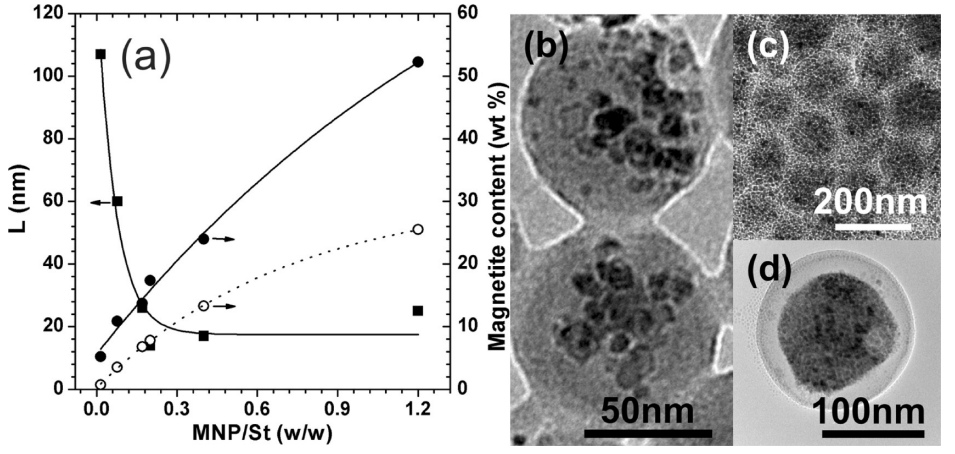

Figure 8. (a) Effect of MNP dose ratio on the thickness of MSPB. Key: (■) brush thickness *L*; magnetite amount in MSPB as determined (●) by TGA and (○) in theory. (b) MSPB with magnetite content 10.9 wt %. (c) TEM image of a MNP clusters and (d) MSPB with a high magnetite content of 52.3 wt %.

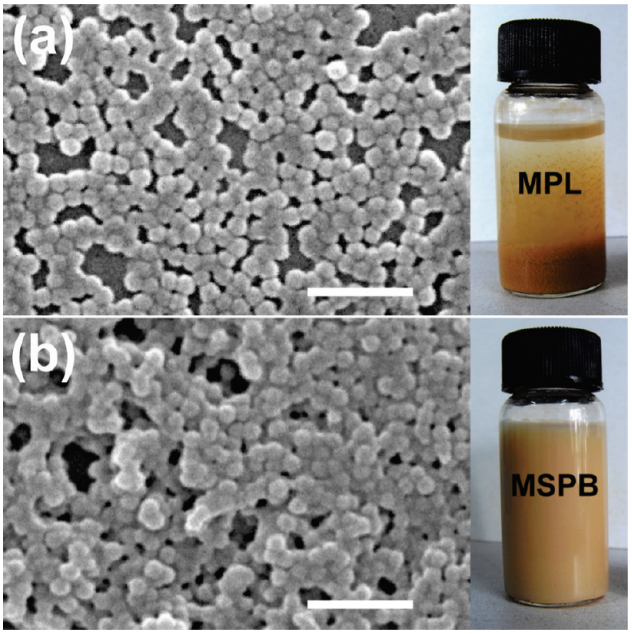

Figure 9. SEM image and optical photo of (a) MPL and (b) MSPB (sample A5, Table 2) after dialysis. The scale bar in SEM images represents 1 μm.

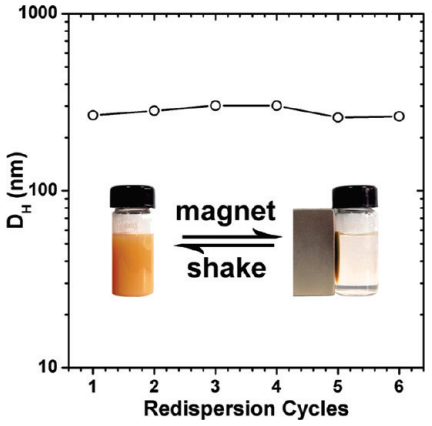

Figure 10. Size of the MSPB after several cycles of aggregation by magnet (NdFeB, 0.5 T) and redispersion as determined by dynamic light scattering (DLS), inset photos show the aggregation and redispersion of MSPB.

is attributed to the spherical PAA brushes on the core surface which provide, especially at high pH, both steric hindrance and electrostatic repulsion.

Both MPL and MSPB were collected by a strong permanent magnet (NdFeB, 0.5T). SEM images (Figure 9) showed that both sediments have a narrow size distribution. Although the MSPB particles seem sticky and adherent each other at dry state, it is still able to redisperse in water by slight shaking.

4.2. Redispersibility. In order to study the redispersibility, MSPB were repeatedly aggregated by a 0.5T magnetic field, and then redispersed for 5 min by untrasonication after removal of the external magnetic field. The average particle size is hardly changed within the experimental error after six cycles of aggregation and redispersion as determined by dynamic light scattering (Figure 10), which reflects the excellent redispersibility of MSPB.

Two factors may affect the redispersibility of MSPB. First, the electrostatic repulsions provided by carboxyl groups

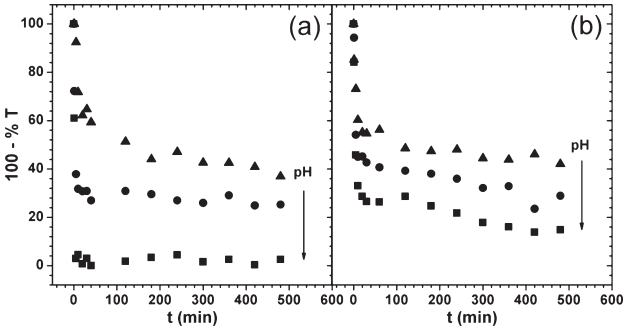

Figure 11. Turbidity as a function of separation time with external magnetic field (NdFeB, 0.5 T) for MSPB with magnetite content (a) 52.3 wt % and (b) 24.0 wt %. Key: (▲) pH = 9.0, ionic strength of 10 mM; (●) pH = 5.0, ionic strength of 10 mM; (■) pH = 3.0, ionic strength of 10 mM.

hinder the entanglement of PAAs among MSPB after collecting by magnet which should enhance the redispersibility of MSPB. Second, superparamagnetism of MSPB ensures the redispersibility. Although the magnetization of MNP decreased after encapsulation into PS core, the MPL and MSPB were still superparamagnetic. Therefore, when magnet was removed after collection, their magnetism lost would be helpful for dispersion of MSPB into water again.

4.3. Control of Separation. The separation of MSPB by external magnetic field was observed by colorimetry (Figure 11). The original turbidity of MSPB solution at pH = 9.0 without external magnetic field was set as 100 (%T) and that of water as zero.

As shown in Figure 11a, MSPB with magnetite content of 52.3 wt % at pH 3.0 were separated most fast and completely. Their suspension became totally transparent after 20 min. At pH 3.0 carboxyl groups in PAA of MSPB did not dissociate to form effective electrostatic repulsion between PAAs and MSPB (Figure 6b). As a result, MSPB shrank and became easy to separate. Upon increasing pH, both the swelling of MSPB and the increased electrostatic repulsion hindered their separating.

When magnetite content decreased to 24.0 wt % (Figure 11b), the separating of MSPB at different pH values became more slowly and incompletely compared to those with high magnetite content. Obviously, high magnetite content and low pH value are favorable for the magnetic separation of MSPB. Therefore, the separation of MSPB can be well controlled by modulating the magnetite content or adjusting pH value.

Nanosized MSPB open the way of many potential applications for SPB, such as catalysis,[9,11] protein immobilization[76,77] and magnetic field-guided drug delivery.[78] Quick magnetic response and good redispersibility guarantee the easy recycling of MSPB for industrial applications.

Conclusions

A novel approach has been developed to introduce magnetic control into spherical polyelectrolyte brushes to achieve the recovery and controllable delivery. Magnetic spherical polyelectrolyte brushes (MSPB) were prepared by photoemulsion polymerization using magnetic polystyrene latices (MPL) as core where the magnetite nanoparticles modified by oleic acid (MNP) were embedded. The MNP were synthesized via coprecipitation method and MPL by miniemulsion polymerization. The fabricated MSPB are narrowly dispersed, superparamagnetic and redispersible after aggregating by external magnetic field. The thickness of MSPB can be controlled by the dose of monomer AA.

Upon increasing the MNP content the brush thickness on MSPB decreases significantly due to the possible inhibition of MNP to the grafting of photoinitiator. Optimal MSPB with high content of MNP were prepared by turning MNP to clusters and using KPS as initiator. Separation process can be well controlled by adjusting magnetite content and pH.

This approach opens the way for the cost-effective applications of SPB in catalysis, wastewater treatment, protein separation, magnetic field-guided drug delivery, disease diagnosis/treatment, and magnetic resonance imaging.

Acknowledgment. We gratefully acknowledge the National Natural Science Foundation of China (No. 20644003, 20774028), the National Special Fund for State Key Laboratory of Bioreactor Engineering (2060204), the Fundamental Research Funds for the Central Universities, the Key Basic Research Project of Shanghai Science and Technology Commission (10JC1403800), and the China Scholarship Council for support of this work.

References and Notes

(1) Rühe, J.; Ballauff, M.; Biesalski, M.; Dziezok, P.; Gröhn, F.; Johannsmann, D.; Houbenov, N.; Hugenberg, N.; Konradi, R.; Minko, S.; Motornov, M.; Netz, R. R.; Schmidt, M.; Seidel, C.; Stamm, M.; Stephan, T.; Usov, D.; Zhang, H. *Adv. Polym. Sci.* **2004**, *165*, 79–150.
(2) Moinard, D.; Borsali, R.; Taton, D.; Gnanou, Y. *Macromolecules* **2005**, *38*, 7105–7120.
(3) Biesalski, M.; Ruhe, J. *Macromolecules* **1999**, *32*, 2309–2316.
(4) Wynveen, A.; Likos, C. N. *Soft Matter* **2010**, *6*, 163–171.
(5) Ballauff, M. *Prog. Polym. Sci.* **2007**, *32*, 1135–1151.
(6) Czeslik, C.; Jackler, G.; Hazlett, T.; Gratton, E.; Steitz, R.; Wittemann, A.; Ballauff, M. *Phys. Chem. Chem. Phys.* **2004**, *6*, 5557–5563.
(7) Wittemann, A.; Haupt, B.; Ballauff, M. *Phys. Chem. Chem. Phys.* **2003**, *5*, 1671–1677.
(8) Lu, Y.; Wittemann, A.; Ballauff, M. *Macromol. Rapid Commun.* **2009**, *30*, 806–815.
(9) Schrinner, M.; Ballauff, M.; Talmon, Y.; Kauffmann, Y.; Thun, J.; Moller, M.; Breu, J. *Science* **2009**, *323*, 617–620.
(10) Lu, Y.; Mei, Y.; Schrinner, M.; Ballauff, M.; Moller, M. W. *J. Phys. Chem. C.* **2007**, *111*, 7676–7681.
(11) Schrinner, M.; Proch, S.; Mei, Y.; Kempe, R.; Miyajima, N.; Ballauff, M. *Adv. Mater.* **2008**, *20*, 1928–1933.
(12) De, M.; Ghosh, P. S.; Rotello, V. M. *Adv. Mater.* **2008**, *20*, 4225–4241.
(13) Kang, Y. S.; Risbud, S.; Rabolt, J. F.; Stroeve, P. *Chem. Mater.* **1996**, *8*, 2209–2211.
(14) Landfester, K. *Adv. Mater.* **2001**, *13*, 765–768.
(15) Laurent, S.; Forge, D.; Port, M.; Roch, A.; Robic, C.; Elst, L. V.; Muller, R. N. *Chem. Rev.* **2008**, *108*, 2064–2110.
(16) Tartaj, P.; Morales, M. D. P.; Veintemillas-Verdaguer, S.; Gonzalez-Carreno, T.; Serna, C. J. *J. Phys. D Appl. Phys.* **2003**, *36*, R182–R197.
(17) Tartaj, P.; Morales, M. P.; Gonzalez-Carreqo, T.; Veintemillas-Verdaguer, S.; Serna, C. J. *J. Magn. Magn. Mater.* **2005**, *290*−*291*, 28–34.
(18) Teja, A. S.; Koh, P. *Prog. Cryst. Growth Charact.* **2009**, *55*, 22–45.
(19) Kim, J.; Lee, J. E.; Lee, S. H.; Yu, J. H.; Lee, J. H.; Park, T. G.; Hyeon, T. *Adv. Mater.* **2008**, *20*, 478–483.
(20) Sun, C.; Lee, J.; Zhang, M. Q. *Adv. Drug Deliver. Rev.* **2008**, *60*, 1252–1265.
(21) Shi, D.; Cho, H. S.; Chen, Y.; Xu, H.; Gu, H.; Lian, J.; Wang, W.; Liu, G.; Huth, C.; Wang, L.; Ewing, R. C.; Budko, S.; Pauletti, G. M.; Dong, Z. *Adv. Mater.* **2009**, *21*, 2170–2173.
(22) Cui, L. L.; Xu, H.; He, P.; Sumitomo, K. K.; Yamaguchi, Y.; Gu, H. C. *J. Polym. Sci., Part A: Polym. Chem.* **2007**, *45*, 5285–5295.
(23) Gong, T.; Yang, D.; Hu, J. H.; Yang, W. L.; Wang, C. C.; Lu, J. Q. *Colloid. Surface. A.* **2009**, *339*, 232–239.
(24) Hoffmann, H.; Landfester, K.; Antonietti, M. *Magnetohydrodynamics* **2001**, *37*, 217–221.
(25) Hong, R. Y.; Feng, B.; Cai, X.; Liu, G.; Li, H. Z.; Ding, J.; Zheng, Y.; Wei, D. G. *J. Appl. Polym. Sci.* **2009**, *112*, 89–98.
(26) Landfester, K.; Ramirez, L. P. *J. Phys: Condens. Matter* **2003**, *15*, S1345–S1361.
(27) Lu, S. H.; Forcada, J. *J. Polym. Sci., Part A: Polym. Chem.* **2006**, *44*, 4187–4203.
(28) Ramirez, L. P.; Landfester, K. *Macromol. Chem. Phys.* **2003**, *204*, 22–31.
(29) Xia, A.; Hu, J.; Wang, C.; Jiang, D. *Small* **2007**, *3*, 1811–1817.
(30) Xu, H.; Cui, L. L.; Tong, N. H.; Gu, H. C. *J. Am. Chem. Soc.* **2006**, *128*, 15582–15583.
(31) Zheng, W. M.; Gao, F.; Gu, H. C. *J. Magn. Magn. Mater.* **2005**, *288*, 403–410.
(32) Jaeyun Kim, H. K. N. L. *Angew. Chem., Int. Ed.* **2008**, *47*, 8438–8441.
(33) Shamim, N.; Hong, L.; Hidajat, K.; Uddin, M. S. *Colloids Surf. B: Biointerfaces* **2007**, *55*, 51–58.
(34) Xu, H.; Tong, N. H.; Cui, L. L.; Lu, Y.; Gu, H. C. *J. Magn. Magn. Mater.* **2007**, *311*, 125–130.
(35) Bakandritsos, A.; Bouropoulos, N.; Zboril, R.; Iliopoulos, K.; Boukos, N.; Chatzikyriakos, G.; Couris, S. *Adv. Funct. Mater.* **2008**, *18*, 1694–1706.
(36) Garcia, I.; Tercjak, A.; Rueda, L.; Mondragon, I. *Macromolecules* **2008**, *41*, 9295–9298.
(37) Gelbrich, T.; Feyen, M.; Schmidt, A. M. *Macromolecules* **2006**, *39*, 3469–3472.
(38) Huang, J. S.; Han, B. Z.; Yue, W.; Yan, H. *J. Mater. Chem.* **2007**, *17*, 3812–3818.
(39) Huang, J. S.; Li, X. T.; Zheng, Y. H.; Zhang, Y.; Zhao, R. Y.; Gao, X. C.; Yan, H. S. *Macromol. Biosci.* **2008**, *8*, 508–515.
(40) Deng, Y. H.; Yang, W. L.; Wang, C. C.; Fu, S. K. *Adv. Mater.* **2003**, *15*, 1729–1732.
(41) Ge, J. P.; Hu, Y. X.; Yin, Y. D. *Angew. Chem., Int. Ed.* **2007**, *46*, 7428–7431.
(42) Mefford, O. T.; Carroll, M.; Vadala, M. L.; Goff, J. D.; Mejia-Ariza, R.; Saunders, M.; Woodward, R. C.; St Pierre, T. G.; Davis, R. M.; Riffle, J. S. *Chem. Mater.* **2008**, *20*, 2184–2191.
(43) Miles, W. C.; Goff, J. D.; Huffstetler, P. P.; Reinholz, C. M.; Pothayee, N.; Caba, B. L.; Boyd, J. S.; Davis, R. A.; Riffle, J. S. *Langmuir* **2009**, *25*, 803–813.
(44) Utech, S.; Scherer, C.; Maskos, M. *J. Magn. Magn. Mater.* **2009**, *321*, 1386–1388.
(45) Utech, S.; Scherer, C.; Krohne, K.; Carrella, L.; Rentschler, E.; Gasi, T.; Ksenofontov, V.; Felser, C.; Maskos, M. *J. Magn. Magn. Mater.* **2010**, *322*, 3519–3526.
(46) Guo, X.; Weiss, A.; Ballauff, M. *Macromolecules* **1999**, *32*, 6043–6046.
(47) Gnanaprakash, G.; Philip, J.; Jayakumar, T.; Raj, B. *J. Phys. Chem. B* **2007**, *111*, 7978–7986.
(48) Lee, S. Y.; Harris, M. T. *J. Colloid Interface Sci.* **2006**, *293*, 401–408.
(49) Qiao, R.; Yang, C.; Gao, M. *J. Mater. Chem.* **2009**, *19*, 6274–6293.
(50) Soler, M.; Alcantara, G. B.; Soares, F. Q.; Viali, W. R.; Sartoratto, P. C.; Fernandez, J.; Da Silva, S. W.; Garg, V. K.; Oliveira, A. C.; Morais, P. C. *Surf. Sci.* **2007**, *601*, 3921–3925.
(51) Vereda, F.; de Vicente, J.; Hidalgo-Alvarez, R. *Langmuir* **2007**, *23*, 3581–3589.
(52) Wang, J.; Chen, Q. W.; Zeng, C.; Hou, B. Y. *Adv. Mater.* **2004**, *16*, 137–140.
(53) Wang, X. M.; Zhang, C. N.; Wang, X. L.; Gu, H. C. *Appl. Surf. Sci.* **2007**, *253*, 7516–7521.
(54) Zhang, L.; He, R.; Gu, H. C. *Appl. Surf. Sci.* **2006**, *253*, 2611–2617.
(55) Goesmann, H.; Feldmann, C. *Angew. Chem., Int. Ed.* **2010**, *49*, 1362–1395.
(56) Wan, M.; Zhou, W.; Li, J. *Synth. Met.* **1996**, *78*, 27–31.
(57) Xu, X. L.; Friedman, G.; Humfeld, K. D.; Majetich, S. A.; Asher, S. A. *Adv. Mater.* **2001**, *13*, 1681–1684.
(58) Xu, X. L.; Friedman, G.; Humfeld, K. D.; Majetich, S. A.; Asher, S. A. *Chem. Mater.* **2002**, *14*, 1249–1256.
(59) Schreiber, E.; Ziener, U.; Manzke, A.; Plettl, A.; Ziemann, P.; Landfester, K. *Chem. Mater.* **2009**, *21*, 1750–1760.
(60) Tiarks, F.; Landfester, K.; Anonietti, M. *Macromol. Chem. Phys.* **2001**, *202*, 51–60.
(61) Liu, X. Q.; Guan, Y. P.; Ma, Z. Y.; Liu, H. Z. *Langmuir* **2004**, *20*, 10278–10282.
(62) Li, L.; Yang, Y.; Ding, J.; Xue, J. *Chem. Mater.* **2010**, *22*, 3183–3191.
(63) Hong, R. Y.; Feng, B.; Liu, G.; Wang, S.; Li, H. Z.; Ding, J. M.; Zheng, Y.; Wei, D. G. *J. Alloy. Compd* **2009**, *476*, 612–618.
(64) Landfester, K.; Bechthold, N.; Tiarks, F.; Antonietti, M. *Macromolecules* **1999**, *32*, 5222–5228.

(65) Asua, J. M. *Prog. Polym. Sci.* **2002**, *27*, 1283–1346.
(66) Guo, X.; Ballauff, M. *Langmuir* **2000**, *16*, 8719–8726.
(67) Guo, X.; Ballauff, M. *Phys. Rev. E* **2001**, *64*, 051406.
(68) Chen, K.; Zhu, Y.; Li, L.; Lu, Y.; Guo, X. *Macromol. Rapid Commun.* **2010**, *31*, 1440–1443.
(69) Luo, Y.; Dai, C.; Chiu, W. *J. Polym. Sci., Part A: Polym. Chem.* **2008**, *46*, 1014–1024.
(70) Antonietti, M.; Landfester, K. *Prog. Polym. Sci.* **2002**, *27*, 689–757.
(71) Landfester, K. *Angew. Chem., Int. Ed.* **2009**, *48*, 4488–4507.
(72) Schork, F. J.; Luo, Y.; Smulders, W.; Russum, J. P.; Butté, A.; Fontenot, K. *Adv. Polym. Sci.* **2005**, 129–255.
(73) Elaissari, A. *Macromol. Symp.* **2009**, *281*, 14–19.
(74) Mori, Y.; Kawaguchi, H. *Colloids Surf. B: Biointerfaces* **2007**, *56*, 246–254.
(75) Sondjaja, R.; Alan Hatton, T.; Tam, M. K. C. *J. Magn. Magn. Mater.* **2009**, *321*, 2393–2397.
(76) Majhi, P. R.; Ganta, R. R.; Vanam, R. P.; Seyrek, E.; Giger, K.; Dubin, P. L. *Langmuir* **2006**, *22*, 9150–9159.
(77) Wittemann, A.; Haupt, B.; Merkle, R.; Ballauff, M. *Macromol. Symp.* **2003**, *191*, 81–88.
(78) Lu, Y.; Hoffmann, M.; Yelamanchili, R. S.; Terrenoire, A.; Schrinner, M.; Drechsler, M.; Moller, M. W.; Breu, J.; Ballauff, M. *Macromol. Chem. Phys.* **2009**, *210*, 377–386.